Research Article

Journal of Physical Organic Chemistry

Received: 11 August 2009, Revised: 8 December 2009, Accepted: 11 December 2009, Published online in Wiley InterScience: 16 March 2010

(www.interscience.wiley.com) DOI 10.1002/poc.1679

Molecular dynamics simulation and MM–PBSA calculations of sickle cell hemoglobin in dimer form with Val, Trp, or Phe at the lateral contact

Hadi Abroshan[a], Hamed Akbarzadeh[a] and Golam Abbas Parsafar[a]*

As the delay time and hence nuclei formation play a crucial role in the pathophysiology of sickle cell disease, MD simulation and molecular mechanics–Poisson–Boltzmann surface area (MM–PBSA) calculations have been performed on three systems of hemoglobin; namely dimer of hemoglobin with valine (Hb S), tryptophan (Hbβ6W), and phenylalanine (Hbβ6F) at β6 position. The structural changes due to these aromatic substitutions are investigated. It is shown that β subunits have significant impact on the differences between a dimer and other crystal structures. Transition from a dimer to polymer for Hb S system affects the donor molecule more than that of the acceptor. In the case of donor and acceptor subunits, the RMSD values are ordered as Hbβ6F > Hbβ6W > Hb S which predicts a larger deviation for the Hbβ6F dimer. It is shown that the formation of stable dimers is in the order of Hbβ6F > Hb S > Hbβ6W, but contribution of the β6 residue in Hbβ6W is more than two other systems. This study shows that the interaction of β6 residue in Hb S is mostly van der Waals type, but in two other systems the electrostatic interaction is also noticeable, especially in the case of Hbβ6W in which the hydrogen bond plays an important role in the association of monomers. Trp and Phe also have a stabilizing van der Waals interaction with a hydrophobic pocket composed of 1β2-10Ala, 1β2-125Pro, 1β2-126Val, and 1β2-129Ala. Our survey shows that the role of $2\beta_1$-85Phe is very important only in the nucleus formation of Hb S, but not for the subsequent processes.

Supporting information may be found in the online version of this paper.

Keywords: molecular disease; molecular dynamics simulation; protein polymerization; protein–protein interaction; sickle cell hemoglobin

INTRODUCTION

Sickle cell anemia reflects a single change in the amino acid building blocks of the oxygen-transport protein, hemoglobin. The beta subunits have the neutral hydrophobic amino acid valine at the position 6 instead of the negatively charged amino acid, Glu.[1,2] The change from a charged to a neutral hydrophobic amino acid creates a sticky patch on the molecular surface that causes aggregation upon deoxygenation. The aggregate is the polymer of sickle cell hemoglobin (Hb S) molecules that assemble in such a way to form seven double stranded fibers.[1–4] For Hb S, the β-6Val residue is intimately involved in a specific lateral contact, at the donor site, which interacts with the acceptor site (hydrophobic EF acceptor pocket) of an adjacent molecule composed predominately of the hydrophobic residue β-85Phe and β-88Leu.[5]

Polymerization is promoted with mutations of β6-Glu → Leu and β6-Glu → Ile, whereas mutation of β6-Glu → Trp (Hbβ6W) and β6-Glu → Phe (Hbβ6F) results in a lower polymerization relative to Hb S, albeit without the delay period characteristic of Hb S polymerization. Adachi *et al*. suggested that Hbβ6W and Hbβ6F form polymers upon deoxygenation by a linear polymerization mechanism without nuclei formation.[6] On the other hand, De Cross *et al*. have demonstrated that 5-bromotryptophan (5-BrTrp) or 5-BrTrp-5-BrTrp derivatives are even more potent inhibitors and suggested that these inhibitors could interact at the surface of the hydrophobic EF pocket and hinder the binding between the donor and the acceptor sites of Hb S.[7]

Studies on characterization of nuclei prior to polymerization may help to define a rational strategy aimed at retarding nuclei formation and inhibiting red cell sickling in patients with sickle cell disease. In recent years, MD simulation has proved to be a valuable tool for studying the dynamic behavior of macromolecular systems,[8–17] and the method is complementary to static X-ray diffraction methods. Especially, for the elucidation of the dynamic pathways of biological transport mechanisms[18–22] and conformational changes,[23–25] MD techniques have recently been very successful in providing additional knowledge concerning complicated biochemical interactions. The molecular

* *Correspondence to: G. A. Parsafar, Department of Chemistry, Sharif University of Technology, Azadi Avenue, Tehran, Iran.*
E-mail: parsafar@sharif.edu

a *H. Abroshan, H. Akbarzadeh, G. A. Parsafar*
Department of Chemistry, Sharif University of Technology, Azadi Avenue, Tehran, Iran

mechanics–Poisson–Boltzmann surface area (MM–PBSA) method was developed to estimate the free energy of ligand–protein and protein–protein interactions.[26] This method combines the calculated interaction energies of MD simulations with the Poisson–Boltzmann calculations of the solvation energy and molecular surface area-based calculations of the non-polar contribution to the solvation free energy.

Substitution of aromatic amino acids like tryptophan and phenylalanine at the β6 position of the hemoglobin molecules inhibits the polymerization and may prevent nuclei formation prior to the polymerization.[6] To explore the structural basis for the striking inhibition of polymerization with a significantly larger residue at β6 (Trp, Phe), molecular dynamics simulations have been performed on dimers of hemoglobin with valine, tryptophan, and phenylalanine at the lateral contact. We have studied the structural changes in the presumed dimers of hemoglobin after replacement of β6-val by tryptophan and phenylalanine relative to Hb S. Interaction energies involved for the residue at β6 position for the three mentioned systems have been evaluated and compared. Energy calculations have also been done to make clear which subunits are more favored to have stabilizing interaction with each other when two hemoglobin molecules are associated. Since association of monomers depends on the solvation energy as well as the interaction energy between monomers in the associated form, free energy calculation using the MM–PBSA method was done and the results have been compared to calculate the relative binding free energy. The contribution of residue β6 to the binding in each of the three systems was evaluated.

MATERIALS AND METHODS

Labeling molecules and subunits

Each system has two hemoglobin molecules associated with each other: one as a donor site is labeled by molecule 1 and the other as the acceptor is labeled by molecule 2. Figure 1 shows how the molecules 1 and 2 and their subunits are assigned. As a paradigm the term $1\beta_2$-6Val implies a valine at the sixth position of the β_2 subunit of the molecule 1.

Setup of the systems

Initial coordinates for the Hb S were taken from the 2.05 Å resolution crystal structure of deoxyhemoglobin S (Protein Data Bank (PDB) code: 2HBS)[27] and to prepare the initial coordinates of Hbβ6W and Hbβ6F approximated models, the side chain of β6 position at lateral contact of the 2HBS has been altered to tryptophan's and phenylalanine's side chains respectively. Other valine residues at β6 positions were not replaced. Like ordinary X-ray structures, the initial structures have no hydrogen atoms; therefore, visual molecular dynamics (VMD)[28] molecular graphics program with CHARMM topology[29] have been applied to add hydrogen atoms. All of the His-20, -45, -50, and -72 of the α subunits and His-77 and -117 of β subunits were modeled as positively charged residues, because these residues are located closely to negatively charged residues.[1,2] All the other histidine residues were modeled as neutral. All Glu and Asp residues were modeled as negatively charged because of the charges of their neighbor residues. The N- and C-terminal residues were modeled as positively and negatively charged, respectively. The entire system had the total charge of $16.0e^{+}$. The resulting structures were surrounded by a rectangular periodic box of TIP3P water molecules[30] that extended to at least 9 Å from the protein atoms to build a 117 Å × 116 Å × 88 Å box for the simulation process. By using the VMD autoionize plugin, sodium and chloride ions were added randomly to the simulation boxes, to neutralize the systems at a physiological salt concentration of ∼100 mM. The total number of atoms for each system was ∼115 000.

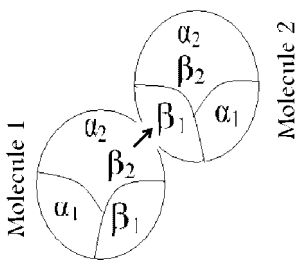

Figure 1. Two hemoglobin molecules along with their subunits. Molecule 1 and molecule 2 are labeled as donor and acceptor, respectively. β_2 of molecule 1 ($1\beta_2$) is the donor subunit and β_1 of molecule 2 ($2\beta_1$) is the acceptor subunit in each dimer

MD simulations

Molecular dynamics simulations were performed using the NAMD package[31] with the CHARMM force field.[29] Before the simulations were carried out, energy of each system was minimized through 25 000 steps. After the minimization, in order to heat proteins, MD runs were carried out at 50, 100, 150, 200, 250, and 300 K for 50 ps at each temperature. MD simulations were continued at 310 K through 12 ns for Hb S, 14 ns for Hbβ6F, and 18 ns for Hbβ6F. All simulations were performed under *NPT* and periodic boundary conditions, using Langevin dynamics with a damping coefficient of 0.5 ps^{-1} and Nose–Hoover Langevin piston[32] with a piston period of 200 fs and a decay time of 100 fs for keeping the temperature and pressure (1 atm) constant respectively. All hydrogen bonds were constrained during the MD simulations using the SHAKE algorithm.[33] The particle mesh Ewald (PME) algorithm[34] was used for the calculation of a long-range electrostatic interaction. The van der Waals forces were treated using a cutoff of 10 Å and the equations of motion were integrated with a time step of 2 fs.

MM–PBSA calculations

The procedure for estimating the binding free energy of the protein–protein complexes is as follows: As many as 100 snapshots have been taken from the last 2 ns of MD trajectory of the donor–acceptor complexes. Unbound proteins were also taken out from the protein–protein complexes' trajectory. The explicit water molecules and ions were removed from the snapshots. The free energy of each species was calculated as follows:

$$G_{tot} = H_{MM} + G_{solv} - T\Delta S_{conf} \quad (1)$$

where H_{MM} is the sum of the terms calculated by molecular mechanics (MM) methods, $E_{bond} + E_{angle} + E_{torsion} + E_{vdW} + E_{elec}$. This term was calculated by using NAMD energy plugin in VMD

with CHARMM force field. Solvation free energy (G_{solv}) is divided into polar and non-polar parts,

$$G_{solv} = G_{solv-np} + G_{solv-pol} \quad (2)$$

The PBSA was used to evaluate the electrostatic solvation energy ($G_{solv\text{-}pol}$).[35] The non-polar contribution ($G_{solv\text{-}np}$), as a linear function of solvent-accessible surface area (SASA) with a probe radius of 1.4 Å, was calculated from

$$G_{solve-np} = \gamma SASA + \beta \quad (3)$$

where the surface tension γ and the offset β were set to the standard values of 0.00542 kcal mol^{-1} Å^{-2} and 0.92 kcal mol^{-1}, respectively.[36] The time-consuming conformational entropy change, $T\Delta S_{conf}$, was not included, because of the large computational overhead and low prediction accuracy. Considering the protein–protein binding of single residue mutants, it has been found that the entropic contribution difference nearly canceled.[37] We have also neglected the entropy term, assuming that it will be very similar for all systems. The binding free energy is approximated by the difference,

$$\Delta G_{bind} = G_{tot}(\text{donor} - \text{acceptor}) - G_{tot}(\text{donor}) - G_{tot}(\text{acceptor}) \quad (4)$$

For the APBS calculation, the CHARMM radii and charges were used. The solvent dielectric, protein dielectric, and solvent radius were set to 80.0, 1.0, and 1.4 Å, respectively. There were no counterions, and the cubic spline window and the V_{acc} sphere density (sdens) were set to 0.3 and 10, respectively. To find the approximate role of the β6 residue in the solvation free energy, the side chain of the mentioned residue was removed from the donor molecule and the PBSA calculation was repeated. The differences between the two results were considered as the polar contribution of solvation free energy for the side chain of β6 residue.

Energy calculations

For each MD trajectory of our simulations, NAMD energy plugin in VMD with CHARMM force field has been applied to calculate the van der Waals and electrostatic interaction energies between different selections in each frame of the simulations. All system preparations, simulation trajectory analysis, and figure preparation were done using VMD. All abbreviations of atom names are based on the CHARMM topology.

RESULTS

Conformational stability of simulations

To investigate the structural behavior of the proteins and test the stability of simulations, we have calculated the root-mean square deviation (RMSD) of the atoms in the backbone of the proteins from the starting structures. As Fig. 2 shows, Hb S dimer reaches the equilibrium state sooner than two other dimers (approximated models of Hbβ6W and Hbβ6F). The average RMSD values for Hb S, Hbβ6W, and Hbβ6F systems within the last 2 ns of the simulations are 3.94, 6.00, and 6.62 Å, respectively. Due to the mutations which have taken place in the active site of the associated hemoglobin molecules, the more needed time for reaching the relative equilibrium state

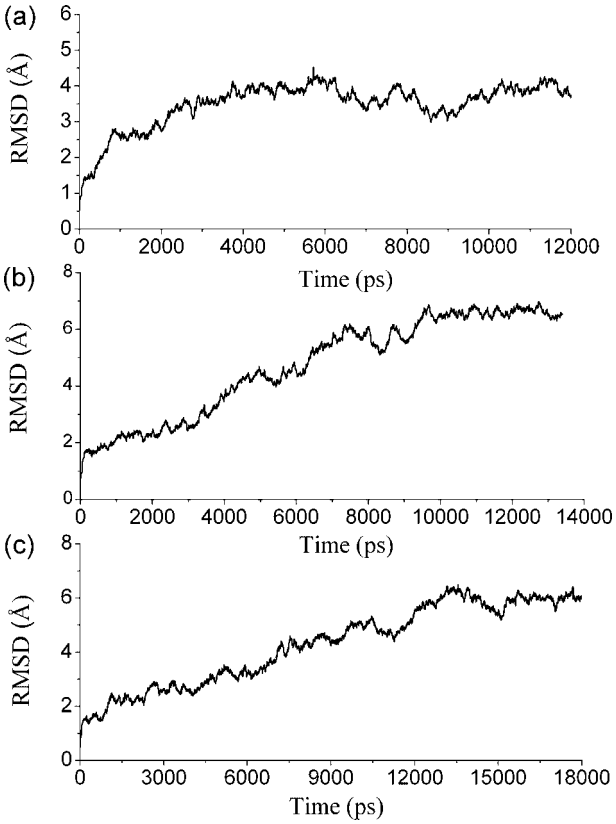

Figure 2. Evolution of root-mean square deviation (RMSD) of the atoms in the backbone of the proteins over time from the initial structure for: (a) Hb S, (b) Hbβ6F, and (c) Hbβ6W

and high values of RMSD for Hbβ6W and Hbβ6F systems relative to Hb S were predictable.

In each molecule, the α subunits usually show less RMSD than the β subunits which is in agreement with previous reports for Hb A and Hb S.[38,39] Since the PDB file of Hb S dimer has been obtained from crystallographic data, such results may indicate that for the Hb S system, the position of the α subunits will change less than that of the β subunits when new monomers are added to the dimer to form a polymer. On the other hand, in this study Hbβ6W and Hbβ6F approximated models have been constructed using crystallographic data of Hb S; therefore, we may conclude that for three systems, the α subunits undergo less changes during the association of dimers for the formation of a polymer. In the other words, deviation of the β subunits may be the main source of structural differences of three systems in the crystal state. This suggestion should be tested by analysis of crystallographic data for Hbβ6W and Hbβ6F. As shown in Table 1, each subunit in different systems has a different value of RMSD. In the Hb S system, $2\alpha_1$, $2\alpha_2$, and $1\alpha_2$ have the least value of RMSD and $1\beta_1$ has the highest value. In the Hbβ6W system, $2\alpha_1$ and $2\alpha_2$ have the least and $1\beta_1$ and $1\beta_2$ have the highest value of RMSD. In the Hbβ6F system, $2\alpha_1$ and $1\alpha_2$ have the least and $1\beta_1$ and $1\beta_2$ have the highest value of RMSD. In all three systems, $1\beta_1$ subunit has a high value of RMSD which may reveal some points about the structural differences between the dimer and polymer states of sickle cell hemoglobin. This table clearly shows that the value of RMSD for subunits of the donor hemoglobins in the Hbβ6W is higher than those for subunits of

Table 1. Average root mean square deviation (RMSD) within the last 2 ns of the simulation for different subunits and their dimers for the three systems

	Hb S	Hbβ6W	Hbβ6F
$2\alpha_1$	1.07	0.95	1.15
$2\beta_1$	1.49	1.77	1.25
$2\alpha_2$	1.08	0.92	1.30
$2\beta_2$	1.85	1.50	1.91
$1\alpha_1$	1.94	1.56	1.42
$1\beta_1$	2.62	1.89	2.04
$1\alpha_2$	0.95	1.72	0.96
$1\beta_2$	1.33	2.27	1.97
$2\alpha_1 2\beta_1$	1.56	1.91	1.60
$2\alpha_1 2\alpha_2$	2.34	2.62	4.47
$2\alpha_1 2\beta_2$	3.75	3.18	4.74
$2\alpha_2 2\beta_1$	1.99	2.17	2.94
$2\beta_1 2\beta_2$	2.90	3.11	3.49
$2\alpha_2 2\beta_2$	2.09	2.22	2.62
$1\alpha_1 1\beta_1$	2.60	2.26	2.13
$1\alpha_1 1\alpha_2$	2.47	2.65	2.70
$1\alpha_1 1\beta_2$	2.82	3.37	3.85
$1\alpha_2 1\beta_1$	2.27	2.59	2.41
$1\beta_1 1\beta_2$	2.61	2.70	3.34
$1\alpha_2 1\beta_2$	1.69	2.32	2.29
$1\beta_2 2\beta_1$	1.82	2.36	2.80
1	3.00	3.44	4.35
2	2.66	3.59	2.86

The value of RMSD for molecule 1 and molecule 2 are also given.

the acceptor molecules. This is also true for the β subunits of Hbβ6F. It is worthy to note that in such systems, the donor subunit ($1\beta_2$) also has a high RMSD value. It is also interesting to consider that for the Hb S system $1\beta_2$ subunit has the least RMSD value among all the β subunits. The average values of RMSD for all subunits of Hb S, Hbβ6W, and Hbβ6F systems are 1.54, 1.57, and 1.50 Å respectively. This result along with the data of Table 1 show that the value of RMSD for the entire Hb S, Hbβ6W, and Hbβ6F dimers are clearly larger than those of the eight subunits and the mentioned average values. These results imply that the subunits changed their relative positions in keeping with the tertiary structures.

The RMSD value for the various dimers of subunits indicates which dimers of subunits in the solution are structurally different with or similar to those in the crystal structure of Hb S. A high value of RMSD refers to more variant relative to a crystal of Hb S and a low value compared to those dimers that have relatively similar structures in both crystal and dimer in solution. It is interesting to note that these values for the Hbβ6F system are usually more than those for two other systems. The average values of RMSD for subunit dimers of Hb S, Hbβ6W, and Hbβ6F are 2.38, 2.57, and 3.03 Å respectively. In the case of $1\beta_2 2\beta_1$ (donor and acceptor subunits), the values are ordered as Hbβ6F > Hbβ6W > Hb S which predicts the difference in the donor and acceptor subunits of Hbβ6F is larger if two hemoglobins form a dimer. The RMSD results for the separated molecules 1 and 2 have also been shown in Table 1 which shows that for the Hbβ6W system they have a similar value, but for two other systems molecule 1 has a higher value, compared to molecule 2. This may suggest that the transition of dimer to polymer for Hb S system affects the donor molecule more than that of the acceptor. On the other hand, it may be concluded from the approximated model that replacement of valine by phenylalanine affects the donor molecule more than the acceptor; however, the replacement by tryptophan affects both of them, equally.

In order to find the structural changes after the aromatic mutations, the average residue-based RMSD was calculated within the last 2 ns of simulations, compared to the initial coordinates (Fig. 3). The largest deviations usually occur in the terminal and loop regions between the α-helices. For all three systems, the relative position of α-helices in a subunit is changed, although there is no significant change in the overall folding pattern. In both α and β subunits, the CD loop shows the largest deviation compared to other loops which is based on the length of the loop that is allowed to vary.

For the three systems, the root-mean square fluctuations (RMSFs) of C_α for different residues were calculated within the last 2 ns of simulations and compared with the equivalent RMSF derived from the B-values in two HbS crystal. Both experimental and computational results show that in the three systems the largest deviations occur in the terminal and loop regions, which are experimentally known to be the most flexible regions. A major difference observed between the RMSF derived from the B-factor and that computed from the simulation result is that the peak values of the RMSF for the loop are higher in the simulation than in the crystal structure. This may be due to the constraints on loop mobility of the crystal which are removed for the proteins in the water box of simulations. It should be noted that for other regions, RMSF derived from the B-values and that computed from the simulation results are similar to some extent. In Table 2 averages of C_α-RMSF for eight subunits in the three systems have been presented. This table indicates that for dimers of three systems, α subunits usually have less fluctuation compared to β subunits. On the other hand, RMSF derived from the B-factor of two HbS shows that there is approximately no significant difference between different types of subunits.

Free energy calculation

Binding free energy calculations provide the qualitative analysis for the effects of residue replacement on protein–protein binding interaction. The results of the MM–PBSA energy terms are presented in Table 3. The MM–PBSA analysis allows us to separate the total free energy of binding into the electrostatic, van der Waals, and solute–solvent interactions, and thereby provides additional insights into the physics of the acceptor–donor association process. As shown in Table 3, electrostatic interaction (ΔH_{MM}^{elec}) plays a very important role in the dimerization. When the ΔH_{MM}^{elec} term is neglected, binding free energy of Hbβ6W will be -18 kcal mol^{-1}, while for the other two systems it is approximately zero. Taking into account the different energy terms we may conclude that two molecules, donor and acceptor, are more apart in the Hbβ6W. Such a conclusion is in accordance with $\Delta G_{solv-pol}$ given in Table 3. The value of $\Delta G_{solv-pol}$ for Hbβ6W is

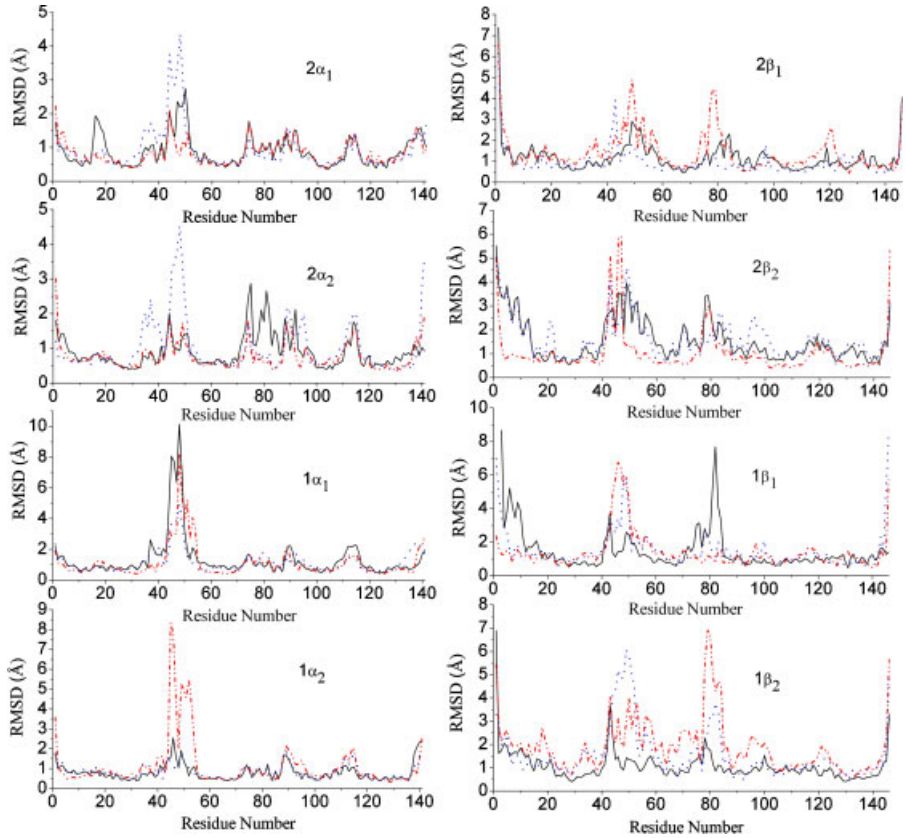

Figure 3. Residue-based root-mean square deviation (RMSD) obtained from MD simulation versus the residue number for different subunits of Hb S (—), Hbβ6F (. . .), and Hbβ6W (– . . .)

noticeably small, compared to that for the two other systems. This may indicate that in Hbβ6W, the loss of protein surface during the association process is less than that for the other two systems. Considering water molecules and the residue at β6 position, the RDF graph also supports such an indication (Fig. 4). For all systems, it may be concluded that the fist layer is formed at a similar distance (∼4 Å), but for Hbβ6W the number of water molecules is more than that of the other two systems. This conclusion is a reasonable result since tryptophan is more polar than valine and phenylalanine which allows water molecules to be more closer to it. Concisely, Table 3 predicts favorable dimerization of hemoglobin in the following order: Hbβ6F > Hb S > Hbβ6W. The contribution of side chain of 1β6 residue in free energy is also presented in Table 3. Although the value of ΔH_{MM}^{elec} could be elucidated on the basis of the dipolar character of the side chains, its value in the case of Hbβ6W can be explained via the hydrogen bond formation which is explained in the next section. The value of $\Delta G_{solv-pol}$ term can be justified as follows: valine is a hydrophobic amino acid which cannot interact with water molecule electrostatically. Based on the RDF graph, tryptophan interacts with more water molecules in the complex state, but phenylalanine is more buried and hence it does not interact with as many water molecules in the complex state. It is also interesting to note that in Hbβ6W, the contribution of 1β6 residue to the free energy is more than in the other two systems.

Table 2. Average value of C_α-RMSF for eight subunits of all three systems

	Hb S	Hbβ6W	Hbβ6F	B-factor
$2\alpha_1$	0.74	0.65	0.72	0.84
$2\beta_1$	0.91	0.82	0.77	0.79
$2\alpha_2$	0.67	0.72	0.65	0.78
$2\beta_2$	0.87	0.98	0.93	0.82
$1\alpha_1$	0.77	0.83	0.87	0.85
$1\beta_1$	0.93	0.90	1.07	0.77
$1\alpha_2$	0.65	0.74	0.62	0.77
$1\beta_2$	0.81	0.81	0.96	0.79

The calculated C_α-RMSF based on the B-factor for Hb S crystal is also presented. Temperature factor flexibility calculated as $(3B/8\pi^2)^{1/2}$, where B is the temperature factor.

Interactions of residue at β6 position

The van der Waals and electrostatic interactions were computed to investigate the forces which lead to the most stable conformation. In the Hb S system with Val at 1β6 position in lateral contact four major interactions were detected. Trajectory analyses show that $2\beta_1$-73Asp, $2\beta_1$-84Thr, $2\beta_1$-85Phe, and $2\beta_1$-88Leu have more stabilizing interactions with $1\beta_2$-6Val than with the others. As shown in Fig. 5, with the exception of $2\beta_1$-73Asp, for other mentioned residues, interaction is predominantly van der Waals-type and the electrostatic interaction does not contribute much. However,

Table 3. Binding free energy components for the donor–acceptor complex by using the MM–PBSA method

System	ΔH_{MM}^{vdW}	ΔH_{MM}^{elec}	$\Delta G_{solv-np}$	$\Delta G_{solv-pol}$	ΔG_{tot}^{a}	$\Delta\Delta G_{tot}^{b}$	%
HbS-HbS	−39.16	−184.93	−5.82	45.04	−184.87 (3.70)	0	—
Hbβ6W-Hbβ6W	−36.81	−152.34	−5.85	24.69	−170.30 (3.21)	+14.57	—
Hbβ6F-Hbβ6F	−49.39	−199.93	−7.93	58.16	−199.09 (4.24)	−14.22	—
HbS-HbS[c]	−5.84	−0.10	−0.60	1.59	−4.95 (0.84)	—	2.68
Hbβ6W-Hbβ6W[c]	−10.05	−4.37	−0.86	3.88	−11.46 (0.72)	—	6.73
Hbβ6F-Hbβ6F[c]	−8.02	−1.97	−0.55	7.56	−2.96 (0.50)	—	1.49

All energies are in kcal mol^{-1}. Statistical errors are given in parentheses. In the last column the contribution of 1β6 residue in free energy is given as percentage of ΔG_{tot}^{a}.

[a] $\Delta G_{tot} = \Delta H_{MM}^{vdW} + \Delta H_{MM}^{elec} + \Delta G_{solv-np} + \Delta G_{solv-pol}$

[b] $\Delta\Delta G_{tot} = \Delta G_{tot}(\text{system}) - \Delta G_{tot}(\text{Hb S})$

[c] Systems without side chain of 1β6 residue.

for 2β_1-73Asp the van der Waals and electrostatic contributions are comparable. Results show that valine has more stabilizing interaction with 2β_1-85Phe than with the other residues, as reported by others.[40,41] On the other hand, experimentally 2β_1-85Phe should have a higher interaction energy than 2β_1-88Leu with 1β_2-6Val,[42,43] which is in accordance with our result. Harrington *et al*. have shown that the lateral contact also includes hydrophilic interactions and bridging water molecules at the periphery of the contact.[27] Simulation of Hb S has shown that there are some water molecules which can form bridging hydrogen bonds between two tetramers in the lateral contact. As shown in Fig. 6, at 1β_2-6Val one water molecule forms a bridging hydrogen bond between two main-chain carbonyl oxygens of 2β_1-84Thr and 1β_2-6Val. Trajectories also presented that bridging hydrogen bonds between the following pairs could be possible: (2β_1-65Lys, 1β_2-79Asp), (2β_1-66Lys, 1β_2-5Pro), (2β_1-66Lys, 1β_2-8Lys), (2β_1-66Lys, 1β_2-9Ser), (2β_1-66Lys, 1β_2-12Thr), (2β_1-69Gly, 1β_2-4Thr), (2β_1-73Asp, 1β_2-4Thr), and (2β_1-87Thr, 1β_2-123Thr).

For the Hbβ6W system, the van der Waals and electrostatic interaction energies between the side chain of Trp at 1β6 position in lateral contact and 2β_1-73Asp, 2β_1-84Thr, 2β_1-85Phe, 2β_1-87Thr, and 2β_1-88Leu were computed and presented in Fig. 7. Trajectory analysis has shown that a hydrogen bond formation between the main-chain carbonyl oxygen of 2β_1-84Thr and HE1 atom of 1β_2-6Trp is favored. The HE1 atom of 1β_2-6Trp

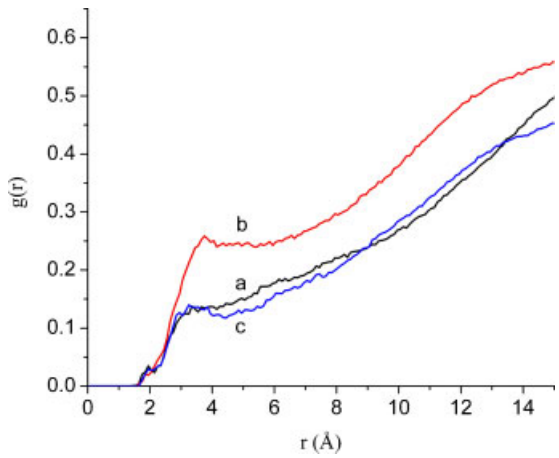

Figure 4. Radial distribution function $g(r)$, for water molecules with respect to 1β6 residue for (a) Hb S, (b) Hbβ6W, and (c) Hbβ6F, respectively

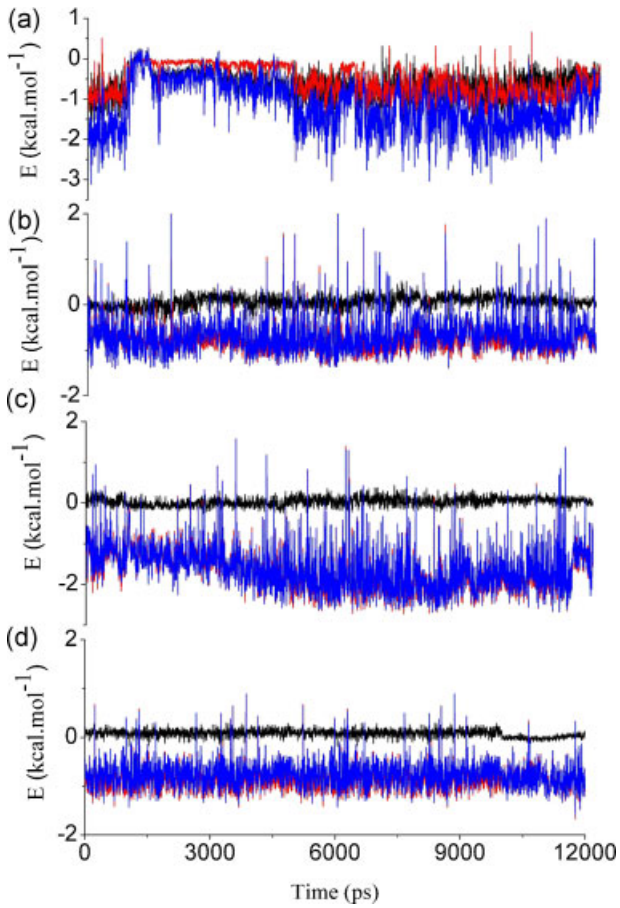

Figure 5. Interaction energy (kcal mol^{-1}) of residue (a) 2β_1-73Asp, (b) 2β_1-84Thr, (c) 2β_1-85Phe, and (d) 2β_1-88Leu and side chain of 1β_2-6Val as a function of simulation time (ps). Black, red, and blue indicate electrostatic, van der Waals, and total energy, respectively

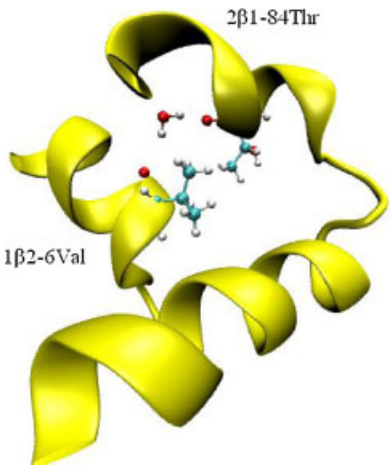

Figure 6. Formation of a bridging hydrogen bond between two main-chain carbonyl oxygens of 2β1-84Thr and 1β2-6Val in the Hb S system

can also form another hydrogen bond with the OG1 atom of $2\beta_1$-87Thr, but because of the side chain's dynamics of $2\beta_1$-87Thr around the CA—CB bond which keeps it far away from $1\beta_2$-6Trp, this interaction is not as strong as in the former case. The distance between two atoms taking part in the first mentioned hydrogen bond versus the simulation time is shown in Fig. 8. It seems that interaction of $1\beta_2$-6Trp with $2\beta_1$-84Thr causes parallel shifting of $1\beta_2$ to the EF loop of $2\beta_1$ at least for a α-helix turn. Such a shifting also allows a side chain of $2\beta_1$-77His to form a hydrogen bond with the side chain of $1\beta_2$-4Thr which is absent in the Hb S system. It is worthy to note that the hydrogen bond between $1\beta_2$-6Trp and $2\beta_1$-84Thr makes the helix F distorted from the normal shape. In such a condition, relative to other systems, there is less hydrogen bond interaction between the main-chain carbonyl oxygen of $2\beta_1$-84Thr and the main-chain amine group of $2\beta_1$-88Leu. On the other hand, the bridging hydrogen bond between $2\beta_1$-73Asp and $1\beta_2$-4Thr is replaced by the hydrogen bond between the mentioned residues completely. As the energy calculations show, the average van der Waals interaction energy of $1\beta_2$-6Trp and $2\beta_1$-85Phe is -1.12 kcal mol^{-1}. Although the average van der Waals interaction of $2\beta_1$-88Leu and $1\beta_2$-6Trp is -0.27 kcal mol, the inappropriate electrostatic interaction makes the average of total interaction energy decrease to -0.14 kcal mol^{-1}. Therefore, there is no noticeable interaction between the two mentioned residues, compared to that in Hb S system. There is another important interaction which is absent in the Hb S system: it is the interaction between the side chain of the residue at β6 position and a group of hydrophobic side chains of its own molecule in the A and H helices. The trajectory analysis shows that the hydrophobic side chains of $1\beta_2$-10Ala, $1\beta_2$-125Pro, $1\beta_2$-126Val, and $1\beta_2$-129Ala are close enough to form a stabilizing van der Waals interaction with $1\beta_2$-6Trp. The average van der Waals and electrostatic interactions are -1.00 and 0.06 kcal mol^{-1} respectively, which clearly indicate that the main contribution is of the van der Waals-type, as expected. Two water molecules contribute to form bridging hydrogen bonds among the main-chain carbonyl oxygen of $1\beta_2$-6Trp, NE1 atom of $1\beta_2$-6Trp, hydroxyl group of $1\beta_2$-9Ser, and the main-chain amine group of $2\beta_1$-87Thr (Fig. 9). Trajectories also revealed that formation of the bridging hydrogen bonds between the following pairs could be possible: ($2\beta_1$-66Lys, $1\beta_2$-8Lys), ($2\beta_1$-88Leu, $1\beta_2$-6Trp),

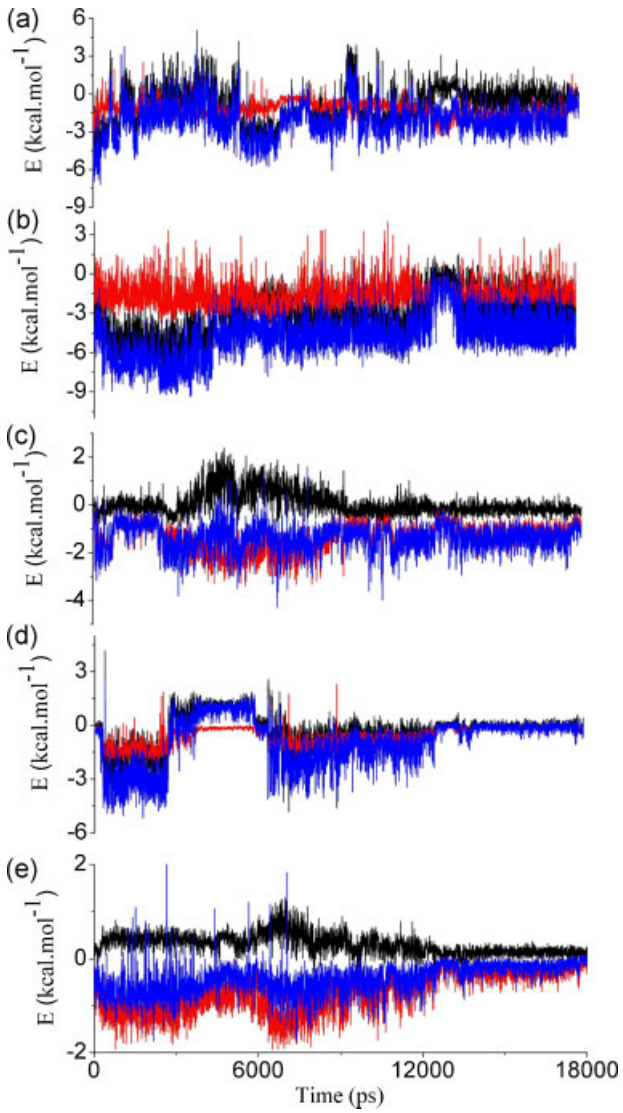

Figure 7. Interaction energy (kcal mol^{-1}) of the side chain of $1\beta_2$-6Trp and (a) $2\beta_1$-73Asp, (b) $2\beta_1$-84Thr, (c) $2\beta_1$-85Phe, (d) $2\beta_1$-87Thr, and (e) $2\beta_1$-88Leu as a function of simulation time (ps) in Hbβ6W system. Black, red, and blue stand for the electrostatic, van der Waals, and total energy, respectively

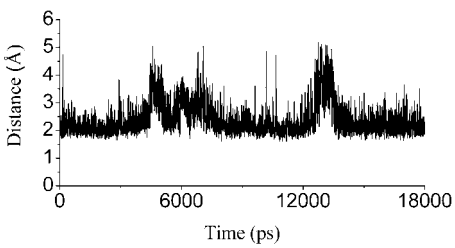

Figure 8. Distance (Å) between two atoms involved in the hydrogen bond formation as a function of simulation time between main-chain carbonyl oxygen of $2\beta_1$-84Thr and HE1 atom of $1\beta_2$-6Trp

and ($2\beta_1$-95Lys, $1\beta_2$-17Lys). The conformation of $1\beta_2$-6Trp relative to the hydrophobic pocket and its own near helices in the equilibrated system is presented in Fig. 10.

For a Hbβ6F system, the interaction energies of $1\beta_2$-6Phe and $2\beta_1$-73Asp, $2\beta_1$-84Thr, $2\beta_1$-85Phe, $2\beta_1$-87Thr, and $2\beta_1$-88Leu residues are presented in Fig. 11. Like the Hbβ6W system, in this case the van der Waals and electrostatic interactions both should be taken into account. The trajectory analysis also shows that in this system $2\beta_1$-84Thr has a stronger interaction with $1\beta_2$-6Phe than with the other residues. The average total interaction energy of $1\beta_2$-6Phe and $2\beta_1$-85Phe is -0.49 kcal mol^{-1} which is 1.13 kcal mol^{-1} less than that of the Hb S system. The average interaction energy between $1\beta_2$-6Phe and $2\beta_1$-88Leu is -0.85 kcal mol^{-1} which is similar to that of the Hb S system. For this case, the electrostatic interaction energy is nearly zero and the interaction is mainly van der Waals-type. Hydrophobic side chains of $1\beta_2$-10Ala, $1\beta_2$-125Pro, $1\beta_2$-126Val, and $1\beta_2$-129Ala contribute to the hydrophobic interaction with the residue at 1β6 position in Hbβ6F system, as well. The average van der Waals and electrostatic interactions are -1.61 and 0.00 kcal mol^{-1}, respectively. The trajectory of simulation shows that the H helix of $1\beta_2$ in Hbβ6W system shifted by half of helix turn and in a parallel direction such that it becomes farther from the Trp side chain. This may lead to the reduction of the van der Waals interaction. One water molecule forms a bridging hydrogen bond among the main-chain carbonyl oxygen of $1\beta_2$-6Phe, hydroxyl group of $1\beta_2$-9Ser, and hydroxyl group of $2\beta_1$-87Thr (Fig. 12). A bridging hydrogen bond between $2\beta_1$-95Lys and $1\beta_2$-16Gly is also possible; on the other hand, bridging hydrogen bond between $2\beta_1$-73Asp and $1\beta_2$-4Thr is replaced with a normal hydrogen bond as well. In a Hbβ6F system, the helix of $1\beta_2$ is close enough to form a hydrogen bond between the side chain of $1\beta_2$-123Thr and the main-chain carbonyl oxygen of $2\beta_1$-83Gly.

In another energy calculation for the three systems, interaction energy of the side chain of the residue at the β6 position and the residues building up the hydrophobic pocket was calculated. Table 4 shows the average interaction energy within the last 2 ns of simulations of the side chain of residue at β6 position for different systems and $2\beta_1$-73Asp, $2\beta_1$-84Thr, $2\beta_1$-85Phe, $2\beta_1$-88Leu, $2\beta_1$-87Thr, and the hydrophobic pocket. For the last

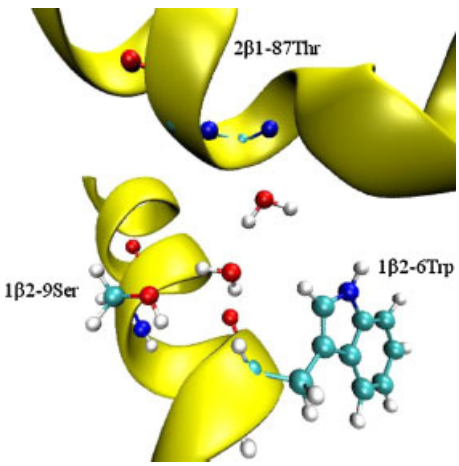

Figure 9. Formation of bridging hydrogen bonds among main-chain carbonyl oxygen of $1\beta_2$-6Trp, NE1 atom of $1\beta_2$-6Trp, hydroxyl group of $1\beta_2$-9Ser, and main-chain amine nitrogen of $2\beta_1$-87Thr

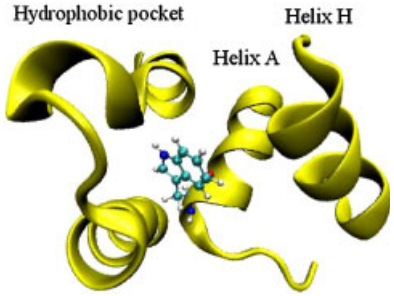

Figure 10. The detailed conformation of 1β2-6Trp relative to hydrophobic pocket and its own near helices (A and H) in the equilibrated simulation time

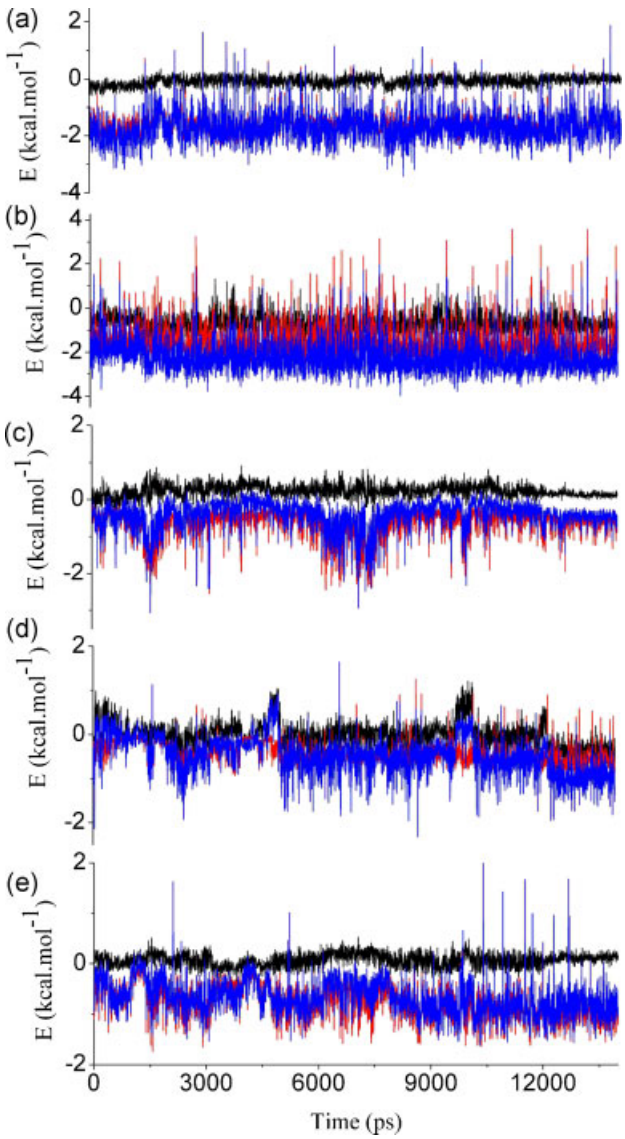

Figure 11. Interaction energy (kcal mol^{-1}) of side chain of 1β2-6Phe and (a) $2\beta_1$-73Asp, (b) $2\beta_1$-84Thr, (c) $2\beta_1$-85Phe, (d) $2\beta_1$-87Thr, and (e) $2\beta_1$-88Leu as a function of simulation time (ps) in Hbβ6F system. Black, red, and blue stand for the electrostatic, van der Waals, and total energy respectively

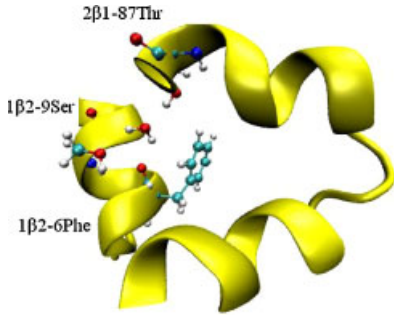

Figure 12. Formation of bridging hydrogen bonds among main-chain carbonyl oxygen of $1\beta_2$-6Trp, hydroxyl group of $1\beta_2$-9Ser, and hydroxyl group of $2\beta_1$-87Thr

calculation, residues 70–90 of $2\beta_1$ were considered as those that build up the mentioned pocket. The interaction energy of subunits $1\beta_2$ and $2\beta_1$, $1\alpha_2$ and $2\beta_1$, $1\beta_1$ and $2\beta_1$, and molecule 1 and molecule 2 are also given in Table 4. These results show the critical role of $2\beta_1$-85Phe in the polymerization of sickle cell hemoglobin. Among the five mentioned residues and other residues in the hydrophobic pocket, $2\beta_1$-85Phe has the strongest interaction with the side chain of valine at the β6 position in Hb S system. On the other hand, this interaction energy is the only one in the Hb S system which is comparable with those of the other two systems. In other words, the interaction energies for other residues of the other two systems are larger than those in the Hb S system. Table 4 shows that in the Hb S system, the dominating interaction with the hydrophobic pocket is the van der Waals-type, but in two other systems the electrostatic interactions should be considered as well, especially in the case of Hbβ6W. This table also shows that in contrast to the Hb S system, in which the hydrophobic pocket residues, $2\beta_1$-73Asp, $2\beta_1$-84Thr, $2\beta_1$-85Phe, and $2\beta_1$-88Leu have dominating interaction energies with the residue at the β6 position, in the case of Hbβ6W and Hbβ6F systems other residues in the hydrophobic pocket contribute to the stabilization energy. Comparison of interaction energy between the residue at β6 position with the hydrophobic pocket in three systems indicates that the interaction may be ordered as Hbβ6W > Hbβ6F > Hb S. When the interaction of $2\beta_1$ and $1\beta_2$ subunits is considered the order will change to Hbβ6F > Hbβ6W > Hb S, but it should be noted that even though the van der Waals interactions for the three systems are similar to some extent, the electrostatic interactions for them are quite different. For the interaction of molecule 1 and molecule 2, the previous ordering changes to Hbβ6F > Hb S > Hbβ6W, which indicates the importance of interactions among other subunits besides $2\beta_1$ and $1\beta_2$ in the probable dimer formation. The electrostatic interaction is the main source of the differences between the two orderings.

Table 4 also presents data of energy calculation for the crystal of Hb S. This table shows that interaction energies of $1\beta_2$-6Val with $2\beta_1$-73Asp, $2\beta_1$-84Thr, $2\beta_1$-87Thr, and $2\beta_1$-88Leu are similar in both crystal and dimer form, but interactions with $2\beta_1$-85Phe are different in the two mentioned states. It is interesting to note that in spite of the dimer form, in crystal state, $1\beta_2$-6Val has more interaction with $2\beta_1$-73Asp than with the other residues. Besides the implication of structural changes, this may imply the very important role of $2\beta_1$-85Phe, only, in the nucleus formation of Hb S, and not in the subsequent processes. There is also no significant difference in the interaction of $1\beta_2$-6Val and the hydrophobic pocket in the two crystal and dimer states. It will be more interesting if interactions of different subunits and also two molecules are considered. For all of them, the van der Waals interaction is the same in crystal and dimer, but in the case of $1\beta_2$-$2\beta_1$, $1\beta_1$-$2\beta_1$, and 1-2, electrostatic interaction energy is

Table 4. The average interaction energy within the last 2 ns of simulations of different parts of the dimers

	73	84	85	87	88	Σ^*	Σ^{**}	$1\beta_2$-$2\beta_1$	$1\alpha_2$-$2\beta_1$	$1\beta_1$-$2\beta_1$	1-2
	−0.54	0.06	0.07	−0.01	0.00	−0.42	−0.26	−67.53	−1.93	−68.09	−184.60
Hb S	−0.76	−0.72	−1.69	−0.07	−0.86	−4.10	−5.27	−27.92	−1.66	−1.40	−30.98
	−1.30	−0.66	−1.62	−0.08	−0.86	−4.52	−5.53	−95.45	−3.59	−69.49	−215.59
	−0.32	−2.79	−0.19	−0.03	0.13	−3.20	−4.76	−108.50	−6.97	0.90	−150.60
Hbβ6W	−1.56	−1.47	−1.12	−0.12	−0.27	−4.54	−9.02	−29.23	−0.01	0.00	−28.55
	−1.88	−4.26	−1.31	−0.16	−0.14	−7.75	−13.67	−137.74	−6.98	0.90	−179.16
	0.00	−0.79	0.14	−0.31	0.11	−2.17	−2.32	−136.62	−31.70	−0.21	−201.42
Hbβ6F	−1.61	−1.55	−0.63	−0.58	−0.96	−5.06	−7.10	−31.62	−7.82	0.00	−39.51
	−1.61	−2.34	−0.49	−0.89	−0.85	−7.23	−9.42	−186.27	−39.53	−0.21	−240.94
	−0.64	−0.02	−0.01	0.00	0.01	−0.66	−0.40	−36.43	−0.78	−36.03	−80.86
Cry-HB S	−1.05	−0.72	−0.70	−0.10	−0.95	−3.52	−4.62	−28.64	−3.07	−0.29	−32.00
	−1.69	−0.74	−0.71	−0.10	−0.94	−4.18	−5.02	−65.07	−3.85	−36.32	−112.86

The first five columns on the left show the average interaction energy (kcal /mol^{-1}) between the sixth residue of $1\beta_2$ subunit and different residues at the hydrophobic pocket. Numbers 73, 84, 85, 87, and 88 indicate different amino acids of the $2\beta_1$ subunit. In each system, the first row indicates the electrostatic, second row the van der Waals, and third row the total interaction energies, respectively. Σ^* indicates the summation of the interaction energies of $2\beta_1$-73Asp, $2\beta_1$-84Thr, $2\beta_1$-85Phe, $2\beta_1$-88Leu, and $2\beta_1$-87Thr with the sixth residue on $1\beta_2$ subunit. Σ^{**} shows the interaction energy of the residue at β6 position with the hydrophobic pocket. In this case, the residues 70–90 of $2\beta_1$ were considered as those that build up the mentioned pocket. The quantities $1\beta_2$-$2\beta_1$, $1\alpha_2$-$2\beta_1$, and $1\beta_1$-$2\beta_1$ indicate the interaction energy of different subunits. 1-2 in the last column indicates the energy of interaction of molecule 1 and molecule 2.

completely different. Such results may be because of dimer solvation as well as lack of axial contacts in the dimer form. In the crystal of Hb S, there is an intramolecular hydrogen bond between the side chains of $1\beta_1$-49Asp and $1\beta_1$-146His, but in the dimer of Hb S this bond is absent. The side chain and the carboxyl terminal group of $1\beta_1$-146His form bridging hydrogen bonds with $2\beta_1$-77His and $2\beta_1$-73Asp. In two other systems, subunits $1\beta_1$ and $2\beta_1$ are farther from each other, compared to the Hb S crystal. In the Hb S system, the interaction energy of $1\beta_1$ and $2\beta_2$ is $-69.49\,\text{kcal mol}^{-1}$, while it is nearly zero for the other two cases. This may imply the structural differences of Hbβ6F and Hbβ6W compared to Hb S. In the latter system, two subunits are close enough to interact, but in Hbβ6F and Hbβ6W systems the distance is so long that there is no noticeable interaction. Table 3 shows that in the Hbβ6F system, the interaction energies among other subunits are more significant. In the crystal of Hb S, the EF loop of $2\beta_1$ is close to $1\alpha_2$ in such a way that $1\alpha_2$-34Leu can interact with the loop. Hydrogen bonds between a side chain of $2\beta_1$-79Asp and the main-chain amino group of $1\alpha_2$-50His is also preferred. In the Hbβ6F system, in addition to the mentioned interactions, hydrogen bond formation between the side chains of $2\beta_1$-8Lys and $1\alpha_2$-49Ser is probable as well. In the Hb S system, in addition to the hydrophobic interaction of $1\alpha_2$-34Leu and the EF loop of $2\beta_1$, the bridging hydrogen bonds among $2\beta_1$-80Asn, $2\beta_1$-79Asp, and $1\alpha_2$-40Lys are allowed. In the Hbβ6W system, none of the above-mentioned interactions are present, but conformation of the $1\alpha_2$ relative to $2\beta_1$ is in such a way that the two mentioned subunits interact only electrostatically with more residues.

Other residues involved in lateral contact

In order to compare the lateral contacts which have already been reported[27,44] with our results obtained from molecular dynamics simulation, Table 5 presents the distances (in angstrom) between the contact atoms in Hb S and Hbβ6W crystals and also for the dimers of Hb S, Hbβ6W, and Hbβ6F obtained from the molecular dynamics simulation. There are some similarities as well as dissimilarities between experimental and simulated data. At this point, we are able to find the main interactions which lead two hemoglobin molecules to associate and form a dimer, in the first step, and the others which appear after adding subsequent hemoglobin molecules to the presumed dimers to form the double strands. In agreement with the experimental observation of the Hb S system,[45,46] there is a lateral contact between 2β1-Asp73 and 1β2-Thr4 which is predominately a hydrogen bond formation between the two mentioned residues. In the other two systems also such a hydrogen bond exists, but stronger than that in the Hb S dimer. Compared to other systems, in the Hbβ6W system the distance is the smallest which is an indication for a strong interaction. Distances between $2\beta_1$-Asp79 and $1\alpha_2$-Ser49, $2\beta_1$-Asp79 and $1\alpha_2$- His50, and also $2\beta_1$-Asn80 and $1\alpha_2$-His50 are quite different in the three systems, which is in agreement with the calculated energies. Distance between

Table 5. Distances (Å) between contact atoms of Hb S and Hbβ6W crystals, and for the dimers of Hb S, Hbβ6W, and Hbβ6F

	Hb S[a]					
	Contact 1	Contact 2	Hbβ6W[a]	Hb S[b]	Hbβ6W[b]	Hbβ6F[b]
$2\beta_1$-Lys66 (O) $1\beta_2$-Pro5 (CG)	3.61	3.65*	6.32	3.64	5.73	4.04
$2\beta_1$-Gly69 (C) $1\beta_2$-Pro5 (CG)	3.89	3.96	5.96*	4.32	4.40	4.65
$2\beta_1$-Ala70 (N) $1\beta_2$-Pro5 (CG)	3.83	3.88	5.14*	4.30	4.82	4.57
$2\beta_1$-Ala70 (CB) $1\beta_2$-Val6 (CG2)	3.83	3.82*	8.51 Trp (CG)	3.86	6.37	5.66 Phe (CG)
			7.22 Trp (CD2)		7.76	5.65 Phe (CD2)
$2\beta_1$-Asp73 (OD2) $1\beta_2$-Thr4 (OG1)	3.11	3.01	5.37*	3.69	2.65	3.19
$2\beta_1$-Asp73 (OD2) $1\beta_2$-Val6 (CB)	3.10	3.92*	8.34*	5.06	3.36	4.45
$2\beta_1$-Asp79 (OD2) $1\alpha_2$- Ser49 (CA)	3.46	3.48	10.33*	7.55	15.20	5.08
$2\beta_1$-Asp79 (OD2) $1\alpha_2$- His50 (N)	2.83	2.88	9.55*	8.19	13.39	4.42
$2\beta_1$-Asn80 (CG) $1\alpha_2$-His50 (CD2)	3.65	3.73*	11.14	6.62	16.95	3.96
$2\beta_1$-Gly83 (O) $1\beta_2$-Pro125 (CG)	3.99	4.10	11.85*	4.67	7.98	4.13
$2\beta_1$-Thr84 (O) $1\beta_2$-Val6 (CG1)	3.62	3.72	4.14	3.78	5.19	5.52
$2\beta_1$-Thr87 (CG2) $1\beta_2$-Ala13 (CB)	3.65	4.63	8.84*	4.06	3.97	5.61
$2\beta_1$-Thr87 (OG1) $1\beta_2$-Ala10 (CA)	4.43	3.75	7.59*	4.15	5.09	4.48
$2\beta_1$-Thr87 (CG2) $1\beta_2$-Val126 (CG2)	5.98	3.83	13.32*	7.88	7.15	4.20
$2\beta_1$-Leu88 (CD2) $1\beta_2$-Ser9 (OG)	3.50	3.36	7.04*	4.07	4.73	3.84
$2\beta_1$-Glu90 (OE2) $1\beta_2$-Lys17 (NZ)	5.03	3.49	11.05*	8.80	3.05	3.93
$2\beta_1$-Lys95 (NZ) $1\beta_2$-Lys17 (NZ)	3.93	5.78	8.46*	13.42	7.08	6.35

Residues closer than 4.0 Å are included with distances shown only for those atoms making the closest contact for each residue pair except those designated with an asterisk, for which a closer atom pair is present. Contact 1 and contact 2 refer to the two crystallographically unique lateral contacts in Hb S.

[a] Crystallographic data of References [6] and [27].

[b] Simulation data of present work.

* See References [6] and [27].

$2\beta_1$-Glu90 and $1\beta_2$-Lys17 residues in the Hb S is so long that there will not be any significant bonding between them, unlike in the two other systems.

Salt bridges and intramolecular interaction between different subunits

In the Hb S system, comparison of similar pairs of subunits in the donor and acceptor shows that van der Waals interaction energy is similar, but electrostatic interactions are different (Supporting Information). On the other hand, except for β_1–β_2, the total interaction energy of subunits of the acceptor molecules is larger than that of the donor. In the other two systems, differences in the van der Waals interactions for the subunits are noticeable, mainly for β_1-β_2, β_1-α_2, and α_1-β_2 which indicate the relative closeness of the mentioned subunits. In the Hbβ6W system, except for β_1-α_2 and α_2-β_2, there is stronger interaction between subunits of acceptor molecules, but interestingly when Hbβ6F is considered; excluding β_1-β_2, and α_2-β_2, there will be a stronger interaction between subunits of the donor molecule. Salt-bridges have been shown to play important structural and functional roles in the interactions.[47] It has clearly been shown that number of salt bridges and residue numbers which form salt bridges are different in the three systems and also in the crystal of Hb S (Supporting Information).

DISCUSSION

In this study we have presented structural differences, van der Waals and electrostatic interactions, and free energy calculation for three systems: Hb S, Hbβ6W, and Hbβ6F. The calculated value of RMSD for the dimer of $1\beta_2 2\beta_1$ is ordered as Hbβ6F > Hbβ6W > Hb S. The ordering is in agreement with the calculated interaction energy between $1\beta_2$ and $2\beta_1$ subunits in both van der Waals and electrostatic points of view. Since the most important contact interaction between two hemoglobin molecules takes place between $1\beta_2$ and $2\beta_1$ subunits, the calculated energies along with the value of RMSD and salt bridge results suggest that the association of pairs of strands in Hbβ6F crystal may be different from that in the Hb S crystal as compared to experiments observed for the crystal of Hbβ6W.[44] The time needed to reach the equilibrium state and RMSD value for the whole dimer support this suggestion as well. It should be noted that the suggestion will be precise if the polymerization process of such a hemoglobin type goes through the nuclei formation. In this study, we have also shown that in the Hbβ6W system there is a shifting in the $1\beta_2$ relative to $2\beta_1$. The present study also shows that there are some structural differences between the donor and acceptor hemoglobin molecules in the three systems.

Knowledge of the degree of surface exposure of an amino acid is valuable and it has been used to enhance the understanding of a variety of biological problems, including protein–protein interactions.[42,48] Our study shows that tryptophan and phenylalanine cannot penetrate to the hydrophobic pocket in the same way that valine does as other researches suggested,[6,43] although the interaction of tryptophan and phenylalanine with the hydrophobic pocket is stronger than that for valine in the Hb S system. Compared to other amino acids, tryptophan occurs least frequently in proteins; furthermore, it is often found at protein surfaces or in the vicinity of the membrane–water interface in the case of membrane proteins. This interfacial exposure of tryptophan might suggest a preferential involvement of Trp in the specific protein–protein interactions. Indeed, statistical analysis of protein–protein interaction sites in a representative sample of protein complexes has revealed that tryptophan is the amino acid with the highest propensity for residing in an interface patch, immediately followed by phenylalanine, another aromatic amino acid. The peculiar interfacial preference of tryptophan might result from its profound dipolar character, the π electronic structure of the indole moiety and perhaps cation–π interactions, or from its flat rigid shape.[49–53] It should be noted that in the Hbβ6W and Hbβ6F systems both van der Waals and electrostatic interactions are stronger than those in Hb S system and contribution of Trp to the free energy is significant. These results are in agreement with the experimental observation, according to which 5-bromotryptophan (5-BrTrp) or 5-BrTrp-5-BrTrp can interact more appropriately to inhibit the polymerization of sickle cell hemoglobin.[7]

Free energy calculation results show that Hbβ6F could form dimers more stable than Hb S, but to investigate the suggestion of Adachi *et al.*[6,44] which indicates that when the lateral interactions compel two hemoglobin molecules to associate for forming a dimer, axial interaction could be favored in such a way that no stable dimers of Hbβ6W and Hbβ6F form, and hence free energy calculation of axial contacts is necessary. Based on the above-mentioned suggestion, protein self-assembly would be facilitated by an end-to-end association of the monomers. Since the axial interactions are the same for the three systems, we may anticipate that their single strand structures are similar. However, due to different circumstances involved in the lateral interactions of the three systems, one may expect that the structure of double strands could be different, as the experimental data support such an expectation for Hbβ6W.

REFERENCES

[1] H. F. Burrn, B. Forget, *Hemoglobin: Molecular, Genetics and Clinical Aspect*, W.B. Saunders, Philadelphia, **1986**.
[2] R. E. Dickerson, I. Geis, *Hemoglobin: Structure, Function, Evolution and Pathology*, The Benjamin/Cummings Publishing Co, Menlo Park, **1983**.
[3] J. G. White, *Blood* **1968**, *31*, 561.
[4] J. G. White, *Arch. Intern. Med.* **1974**, *133*, 545.
[5] E. A. Paldan, W. E. Love, *J. Biol. Chem.* **1985**, *260*, 8280.
[6] K. Adachi, P. Konitzer, J. Kim, N. Welch, S. Surrey, *J. Biol. Chem.* **1993**, *268*, 21650.
[7] P. Z. De Cross, P. Sangdee, B. L. Stockwell, L. Kar, E. B. Thompson, M. E. Johnson, B. L. Currie, *J. Med. Chem.* **1990**, *33*, 3138.
[8] S. A. Adcock, J. A. McCammon, *Chem. Rev.* **2006**, *105*, 1589.
[9] M. Karplus, J. Kuriyan, *J. Proc. Natl Acad. Sci. U. S. A.* **2005**, *102*, 6679.
[10] M. Garcia-Viloca, J. Gao, M. Karplus, D. G. Truhlar, *Science* **2004**, *303*, 186.
[11] S. J. Benkovic, S. A. Hammes-Schiffer, *Science* **2003**, *301*, 1196.
[12] F. Pietra, *J. Phys. Org. Chem.* **2009**, *22*, 89.
[13] F. Pietra, *J. Phys. Org. Chem.* **2008**, *21*, 997.
[14] E. Humeres, C. Mascayano, G. Riadi, F. Gonzalez-Nilo, *J. Phys. Org. Chem.* **2006**, *19*, 89.
[15] N. Carrasco, F. Gonzalez-Nilo, M. Caroli Rezende, *J. Phys. Org. Chem.* **2005**, *18*, 128.
[16] M. J. Potrzebowski, S. Kazmierski, S. Olejniczak, J. Helinski, W. Ciesielski, A. Dolle, *J. Phys. Org. Chem.* **2005**, *18*, 602.
[17] C. Yang, X. Zhu, J. Li, K. Chen, *J. Mol. Struct. (THEOCHEM)* **2009**, *907*, 51.
[18] J. Aqvist, V. Luzhkov, *Nature* **2000**, *404*, 881–884.

[19] S. Berneche, B. Roux, *Nature* **2001**, *414*, 73.
[20] B. L. De Groot, H. Grubmuller, *Curr. Opin. Struct. Biol.* **2005**, *15*, 176.
[21] L. R. Forrest, M. S. Sansom, *Curr. Opin. Struct. Biol.* **2000**, *10*, 174.
[22] L. Saiz, M. L. Klein, *Acc. Chem. Res.* **2002**, *35*, 482.
[23] K. Lindorff-Larsen, R. B. Best, M. A. DePristo, C. M. Dobson, M. Vendruscolo, *Nature* **2005**, *433*, 128.
[24] V. Hornak, A. Okur, R. C. Rizzo, C. Simmerling, *Proc. Natl Acad. Sci. U. S. A.* **2006**, *103*, 915.
[25] V. Hornak, A. Okur, R. C. Rizzo, C. Simmerling, *J. Am. Chem. Soc.* **2006**, *128*, 2812.
[26] J. Srinivasan, T. E. Cheatham, P. Kollman, D. Case, *J. Am. Chem. Soc.* **1998**, *120*, 9401.
[27] D. L. Harrington, K. Adachi, W. E. Royer, Jr, *J. Mol. Biol.* **1997**, *272*, 398.
[28] W. Humphrey, A. Dalke, K. Schulten, *J. Mol. Graph.* **1996**, *14*, 33–38.
[29] A. D. MacKerell, Jr, D. Bashford, M. Bellott, R. L. Dunbrack, Jr, J. Evanseck, M. J. Field, S. Fischer, J. Gao, H. Guo, S. Ha, D. Joseph, L. Kuchnir, K. Kuczera, F. T. K. Lau, C. Mattos, S. Michnick, T. Ngo, D. T. Nguyen, B. Prodhom, W. E. Reiher, B. Roux, M. Schlenkrich, J. Smith, R. Stote, J. Straub, M. Watanabe, J. Wiorkiewicz-Kuczera, D. Yin, M. Karplus, *J. Phys. Chem. B* **1998**, *102*, 3586.
[30] W. L. Jorgensen, J. Chandrasekhar, M. L. Madura, J. D. Klein, *J. Chem. Phys.* **1983**, *79*, 926.
[31] J. C. Phillips, R. Braun, W. Wang, J. Gumbart, E. Tajkhorshid, E. Villa, C. Chipot, R. D. Skeel, L. Kale, K. J. Schulten, *Comput. Chem.* **2005**, *26*, 1781.
[32] S. E. Feller, Y. H. Zhang, R. W. Pastor, B. R. Brooks, *J. Chem. Phys.* **1995**, *103*, 4613.
[33] J. P. Ryckaert, G. Ciccotti, H. J. C. Berendsen, *J. Comput. Phys.* **1977**, *23*, 327.
[34] T. Darden, D. York, L. Pedersen, *J. Chem. Phys.* **1993**, *98*, 10089.
[35] N. A. Baker, D. Sept, S. Joseph, M. J. Holst, J. A. McCammon, *Proc. Natl. Acad. Sci. U. S. A.* **2001**, *98*, 10037.
[36] D. Sitkoff, K. A. Sharp, B. J. Honig, *Phys. Chem.* **1994**, *98*, 1978.
[37] I. Massova, P. A. Kollman, *J. Am. Chem. Soc.* **1999**, *121*(36), 8133.
[38] M. Prabhakaran, M. E. Johnson, *Biopolymers* **1993**, *33*, 735.
[39] M. Saito, L. Okazaki, *J. Comput. Chem.* **2007**, *28*, 1129.
[40] K. Adachi, L. R. Reddy, S. Surrey, *J. Mol. Biol.* **1994**, *269*, 31563.
[41] K. Adachi, L. R. Reddy, K. S. Reddy, S. Surrey, *Protein Sci.* **1995**, *4*, 1272.
[42] S. Jones, J. M. Thornton, *J. Mol. Biol.* **1997**, *272*(1), 133.
[43] M. T. Bihoreau, V. Baudin, M. Marden, J. Lacaze, B. Bohn, J. Kister, O. Schaad, A. Dumoulin, S. J. Edelstein, C. Poyart, J. Pagnier, *Protein Sci.* **1992**, *1*, 145.
[44] D. J. Harrington, K. Adachi, W. E. Royer, Jr. *J. Biol. Chem.* **1998**, *273*, 32690.
[45] R. M. Bookchin, R. L. Nagel, H. M. Ranney, *Biochimica. et Biophysica. Acta* **1970**, *221*, 373.
[46] R. M. Bookchin, R. L. Nagel, H. M. Ranney, *J. Biol. Chem.* **1967**, *242*, 248.
[47] D. J. Barlow, J. M. Thornton, *J. Mol. Biol.* **1983**, *168*, 867.
[48] S. Jones, J. M. Thornton, *J. Mol. Biol.* **1997**, *272*(1), 121.
[49] Y. Thielmann, J. Mohrl, B. W. Koenig, T. Stangler, R. Hartmann, K. Becker, H. D. Holtje, D. Willbold, *ChemBioChem* **2008**, *9*, 1767.
[50] C. Landolt-Marticorena, K. A. Williams, C. M. Deber, R. A. Reithmeier, *J. Mol. Biol.* **1993**, *229*, 602.
[51] S. Jones, J. M. Thornton, *J. Mol. Biol.* **1997**, *272*, 121.
[52] D. A. Dougherty, *Science* **1996**, *271*, 163.
[53] W. M. Yau, W. C. Wimley, K. Gawrisch, S. H. White, *Biochemistry* **1998**, *37*, 14713.

